AD-A127 762 SELF-REFLECTING SKEW POLYGONS AND POLYTOPES IN THE 4-DIMENSIONAL HYPERCUBE(U) WISCONSIN UNIV-MADISON MATHEMATICS RESEARCH CENTER I J SCHOENBERG JAN 83 1/1

UNCLASSIFIED MRC-TSR-2467 DAAG29-80-C-0041 F/G 12/1 NL

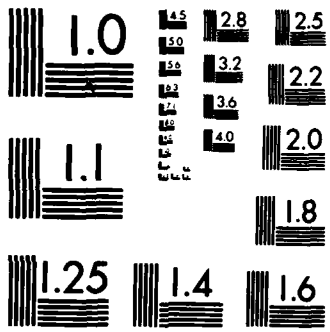
1.0
2.8
2.5
3.2
2.2
3.6
4.0
2.0
1.1
1.8
1.25
1.4
1.6

MRC Technical Summary Report #2467

SELF-REFLECTING SKEW POLYGONS AND POLYTOPES IN THE 4-DIMENSIONAL HYPERCUBE

I. J. Schoenberg

Mathematics Research Center
University of Wisconsin—Madison
610 Walnut Street
Madison, Wisconsin 53706

January 1983

(Received December 8, 1982)

Sponsored by

U. S. Army Research Office
P. O. Box 12211
Research Triangle Park
North Carolina 27709

UNIVERSITY OF WISCONSIN-MADISON
MATHEMATICS RESEARCH CENTER

SELF-REFLECTING SKEW POLYGONS AND POLYTOPES IN THE 4-DIMENSIONAL HYPERCUBE

I. J. Schoenberg

Technical Summary Report #2467
January 1983

ABSTRACT

The papers [2,3,4,5] of the list of References dealt with the following extremum problem: In the hypercube γ_n of R^n we have a k-flat L_k in general position which is reflected by the $(n - 1)$-facets of γ_n, while we continue indefinitely reflecting these reflexions, thereby generating a finite or infinite polytope Π_n^k. Here we assume that

$$1 \leq k \leq n - 1 .$$

The present paper deals with the case when $n = 4$, and when

$$k = 1, k = 2, \text{ and } k = 3 . \tag{1}$$

The main problem is to determine Π_n^k to stay away as much as possible from the center c of γ_n, the main emphasis being the graphic representation of the extremum Π_n^k. This is done for the three cases (1) in Figures 2, 4, and 8. These figures are parallel projections of γ_4 onto our space R^3. The author also made for each of these figures 3-dimensional models made of thin wooden sticks, and my colleagues, in the Fine Arts Department of UW, say that these models qualify as examples of Constructive Art. All of these polygons and polytopes are <u>self-reflecting</u>, meaning thereby that we obtain the entire object by starting from one of its k-facets, and reflecting it successively in the facets of γ_4.

AMS (MOS) Subject Classifications: 51N20, 52A25

Key Words: Extremum problems, billiard ball motions

Work Unit Number 1 (Applied Analysis)

Sponsored by the United States Army under Contract No. DAAG29-80-C-0041.

SIGNIFICANCE AND EXPLANATION

In papers [2,3,4,5] of the list of References the author dealt with certain extremum problems for billiard ball motions in the hypercube γ_n of R^n. Here we study in greater detail the case when $n = 4$, the results being graphically described in the three Figures 2, 4, and 8. The author also made 3-dimensional models corresponding to these figures out of thin wooden sticks.

The responsibility for the wording and views expressed in this descriptive summary lies with MRC, and not with the author of this report.

SELF-REFLECTING SKEW POLYGONS AND POLYTOPES IN THE 4-DIMENSIONAL HYPERCUBE

I. J. Schoenberg

1. INTRODUCTION.

This is a contribution to some geometric aspects of the 4-dimensional hypercube γ_4. Following the pioneering paper [1] of König and Szűcs the author has studied billiard ball motions in a hypercube of R^n in his papers [2, 3, 4, 5]. The main concern is an extremum problem which may be stated as follows.

Let

$$\gamma_n : 0 \leq x_i \leq 1, \quad (i = 1,2,\ldots,n) \tag{1.1}$$

be the measure polytope in R^n. In γ_n we consider a k-dimensional flat $(1 < k < n - 1)$ given parametrically by

$$L_k : x_i = \sum_{j=1}^{k} \lambda_i^j u_j + a_i \quad (i = 1,\ldots,n) , \tag{1.2}$$

such that the point $a = (a_i)$ is interior to γ_n.

We now reflect L_k in the 2n facets $x_i = 0$ and $x_i = 1$ of γ_n whenever L_k strikes them, and keep reflecting these reflexions indefinitely thereby generating a finite or infinite polytope which we denote by Π_n^k. The entire study was made possible by the use of the auxilliary function $\langle x \rangle$ defined by

$$\langle x \rangle = \begin{cases} x & \text{if } 0 \leq x \leq 1 , \\ 2-x & \text{if } 1 \leq x \leq 2 , \end{cases} \quad \langle x + 2 \rangle = \langle x \rangle \text{ for all real } x . \tag{1.3}$$

We may call this the linear Euler spline; it has a zig-zag graph shown in Figure 3 below. By means of it the reflected polytope admits the equations

$$\Pi_n^k : x_i = \left\langle \sum_{j=1}^{k} \lambda_i^j u_j + a_i \right\rangle , \quad (i = 1,\ldots,n) . \tag{1.4}$$

Sponsored by the United States Army under Contract No. DAAG29-80-C-0041.

In general we have the ergodic situation: the polytope Π_n^k is dense in γ_n. As the opposite of ergodicity we assume that there is an open hypercube

(1.5) $$C_\rho : \|x - c\|_\infty < \rho, \quad c = \left(\frac{1}{2}, \frac{1}{2}, \ldots, \frac{1}{2}\right), \quad 0 < \rho < \frac{1}{2},$$

such that Π_n^k does not penetrate into C_ρ, hence such that

(1.6) $$\Pi_n^k \cap C_\rho = \emptyset .$$

However, in order to have a truly n-dimensional situation, we must assume that L_k is in a <u>general position</u>.

<u>Definition 1</u>. <u>We say that</u> L_k <u>is in general position provided that</u>

(1.7) <u>the</u> $n \times k$ <u>matrix</u> $\|\lambda_i^j\|$ <u>has no vanishing minor of order</u> k.

Our problem is to determine, or estimate, the quantity

(1.8) $$\sup \rho = \rho_{k,n}$$

under the assumptions (1.6) and (1.7). In [4, Theorem 1, p. 55] it was shown that

(1.9) $$\rho_{k,n} \geq \frac{1}{2} - \frac{k}{2n} \quad \text{for all} \quad k = 1,2,\ldots,n-1 .$$

It was also shown ([3], and [4, Theorem 2, p.55]) that in (1.9) we have the equality sign for the two extreme values of k:

(1.10) $$\rho_{1,n} = \frac{1}{2} - \frac{1}{2n} = \frac{n-1}{2n}, \quad \text{and} \quad \rho_{n-1,n} = \frac{1}{2} - \frac{n-1}{2n} = \frac{1}{2n} .$$

It was also conjectured in [4, p. 56] that the equality sign holds in (1.9) also for $k = 2,3,\ldots,k-2$, but this has not been established.

Let us look at the simplest cases.

1. If $k = 1$ and $n = 2$, then by (1.10) we have that $\rho_{1,2} = 1/4$, and the polygon Π_2^1 satisfying $\Pi_2^1 \cap C_{1/4} = \emptyset$ is the slanting square of Fig. 1 (a).

2. If $k = 1$ and $n = 3$, then again by (1.10) we have $\rho_{1,3} = 1/3$, while Π_3^1 is the hexagon 123456 which winds its way around the maximal cube $C_{1/3}$, as shown in Fig. 1 (b)

3. Finally we consider the case $k = 2$ and $n = 3$. By (1.10) we have $\rho_{2,3} = 1/6$, and the corresponding polyhedron Π_3^2 is Kepler's regular tetraheron $T = ABCD$ shown in Fig. 1 (c).

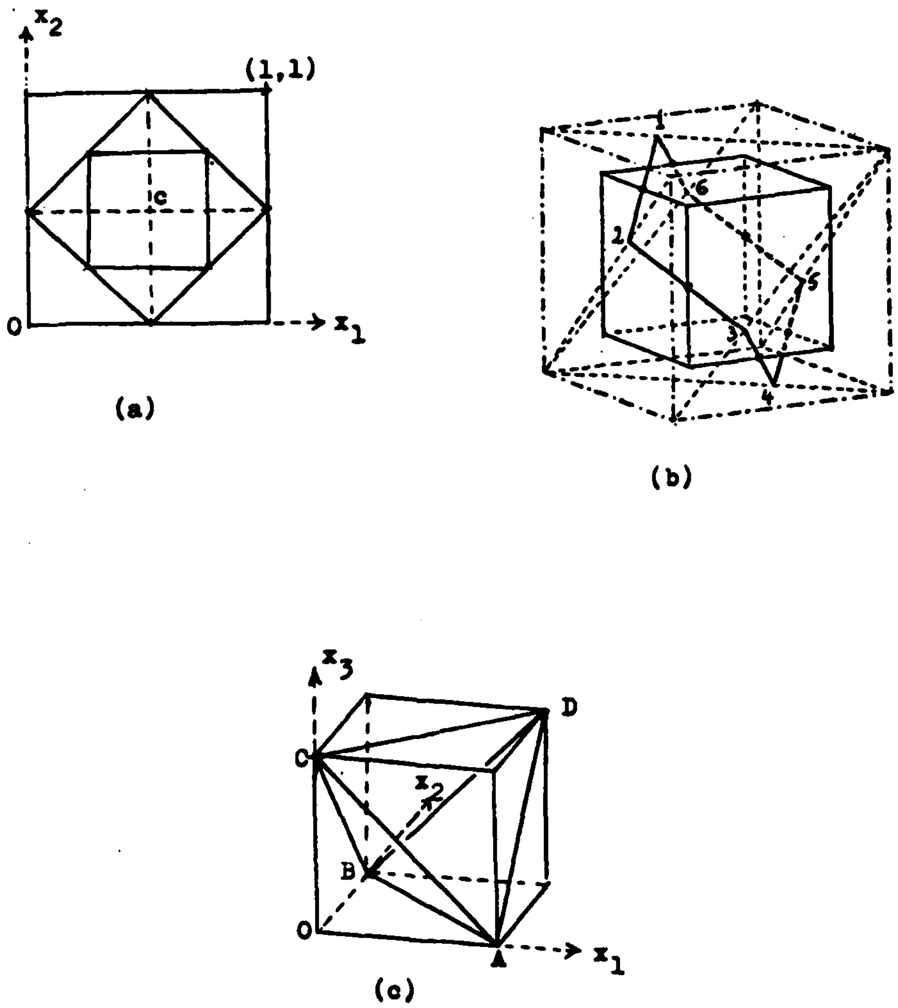

Fig. 1

As in the general case of (1.4) the figures, in all three cases of Fig. 1, are seen to be <u>self-reflecting</u>: starting from any edge, or facet, we obtain by successive reflections the entire figure.

The present paper deals with the simplest higher-dimensional case when $n = 4$, and is divided in two parts. In Part I we discuss the two cases when $k = 1$ and $k = 2$. The general results (1.9) and (1.10) were given for orientation only, and will not be used in Part I. In Part II we discuss the case $k = 3$ using results of our last paper [5].

In both parts the emphasis is on the graphic representation given in Figures 2, 4, 8. These are naturally plane figures, but should be regarded as figures in R^3. These 3-dimensional figures represent parallel projections of γ_4 onto our space R^3. Nevertheless we will often regard them as actually representing γ_4, rather than its projections on R^3.*)

The author also made 3-dimensional models, corresponding to these figures, made out of thin wooden sticks, and the author's colleagues in the Fine Arts Department of the University of Wisconsin say that they qualify as examples of Constructive Art. For further models concerning the finite Fourier series see Chapter 9 of the author's forthcoming book [6].

Perhaps the main contribution of this paper is the second part of Part I corresponding to the case when $k = 2$: The discovery of the skew octahedron $\mathcal{O}$, in γ_4, which is self-reflecting (Fig. 4). It is the analogue in γ_4, for $k = 2$, of Kepler's tetrahedron T of Fig. 1 (c).

Part I. The two cases when $k = 1,2$

2. The "lucky" billiard ball shot for $n = 4$. This was discussed for a general n in [3]. Here we derive it independently for $n = 4$ in

*) Our figures 2, 4 and 8, remind us of the absent-minded teacher who writes A, means B, and should have written C: Our three figures are in R^2, represent objects in R^3, and should really represent objects in R^4.

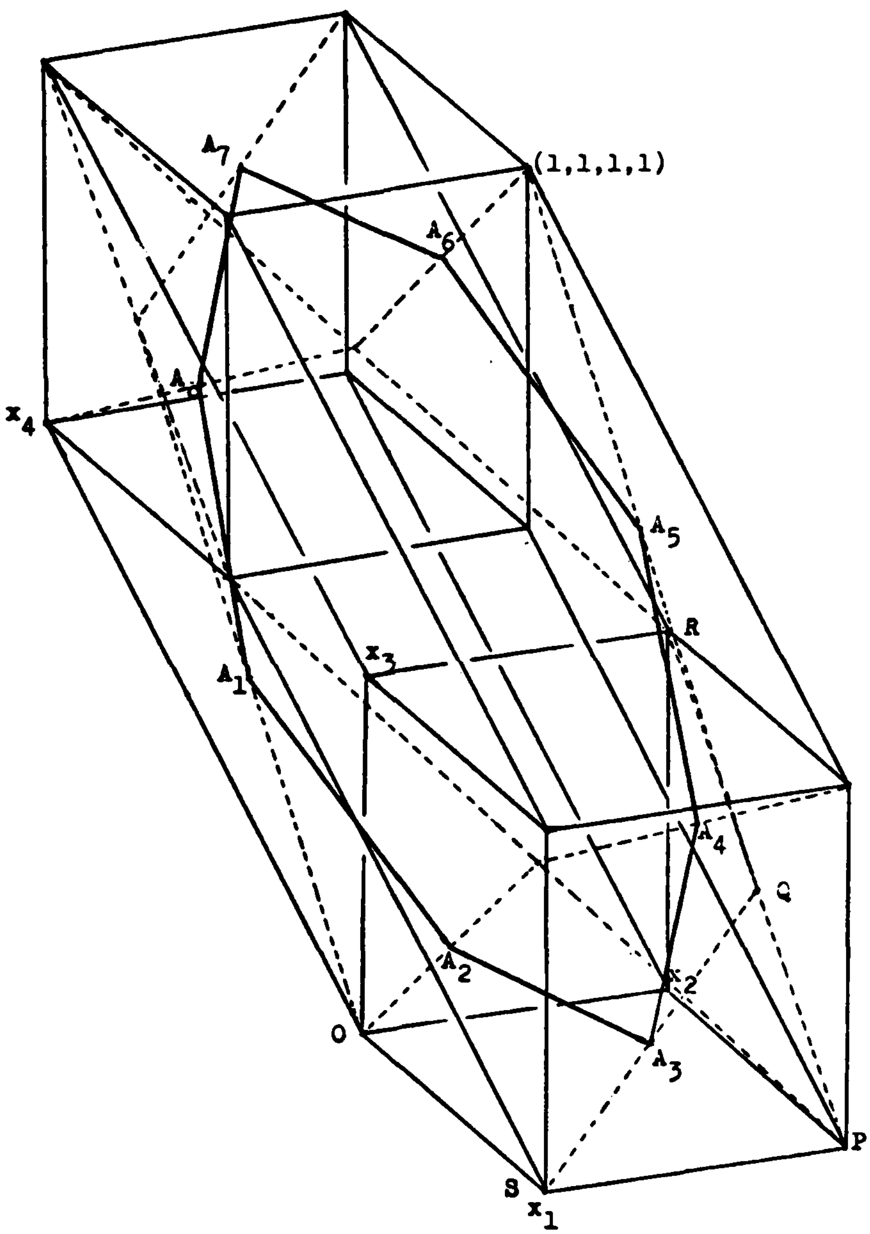

Fig. 2

<u>Theorem 1. The equations</u>

$$x_1 = \langle u\rangle,\ x_2 = \langle u - \tfrac{1}{4}\rangle,\ x_3 = \langle u - \tfrac{2}{4}\rangle,\ x_4 = \langle u - \tfrac{3}{4}\rangle, \quad (0 \le u \le 2) \tag{2.1}$$

<u>define an octagon</u> $\Pi_4^1 = A_0A_1,\dots,A_7$, <u>shown in Fig. 2, having the following properties</u>

1. Π_4^1 <u>is the path of a billiard ball within</u> γ_4.

2. Π_4^1 <u>has no point in common with the open hypercube</u>

$$C_{3/8} : \|x - c\|_\infty < \frac{3}{8}, \quad \left(c = \left(\tfrac{1}{2},\dots,\tfrac{1}{2}\right)\right), \tag{2.2}$$

<u>while the midpoints of the</u> 8 <u>sides of</u> Π_4^1 <u>are in 2-dimensional facets of</u> $C_{3/8}$.

3. <u>We have</u>

$$\rho_{1,4} = \frac{3}{8}. \tag{2.3}$$

According to the definition (1.8) this means the following: <u>If</u> $3/8 < \rho < 1/2$, <u>then every billiard ball path which is initially not parallel to any of the coordinate hyperplanes</u> $x_i = 0$, <u>must penetrate within the open hypercube</u>

$$C_\rho : \|x - c\|_\infty < \rho. \tag{2.4}$$

<u>Proofs of 1 and 2</u>. 1. (2.1) define a closed octagon because the equations (2.1) are linear in each of the eight intervals

$$\frac{i}{4} \le u \le \frac{i}{4} + \frac{1}{4}, \quad (i = 0,1,\dots,7).$$

If we write (2.1) as $x = f(u)$, and denote the vertices by $A_i = f(i/4)$, we find that these vertices are

$$\begin{aligned}
A_0 &= (\ 0\ , 1/4, 2/4, 3/4), & A_4 &= (\ 1\ , 3/4, 2/4, 1/4),\\
A_1 &= (1/4,\ 0\ , 1/4, 2/4), & A_5 &= (3/4,\ 1\ , 3/4, 2/4),\\
A_2 &= (2/4, 1/4,\ 0\ , 1/4), & A_6 &= (2/4, 3/4,\ 1\ , 3/4),\\
A_3 &= (3/4, 2/4, 1/4,\ 0\ ), & A_7 &= (1/4, 2/4, 3/4,\ 1\ ).
\end{aligned} \tag{2.5}$$

That the equations (2.1) define the path of a billiard ball is due to the zig-zag nature of the graph of the function (1.3).

2. That $\Pi_4^1 \cap C_{3/8} = \emptyset$ may be expressed by saying that Π_4^1 is contained in the closed hypercubical box

$$B = \gamma_4 \setminus C_{3/8}. \tag{2.6}$$

That indeed

$$\Pi_4^1 \subset B \tag{2.7}$$

is seen as follows: The four arguments

$$u,\ u-\frac{1}{4},\ u-\frac{2}{4},\ u-\frac{3}{4}\ ,$$

appearing in (2.1), are equidistant with step $h = 1/4$. This implies that at least one of them, $u - (i/4)$ say, is at a distance $\leqq 1/8$ from some integer point j, hence that

$$u - \frac{i}{4} = j + \theta, \qquad (|\theta| \leqq 1/8,\ j \in \mathbb{Z})\ .$$

However, from (2.1) and Fig. 3, we see that we therefore have

$$\text{either}\quad 7/8 \leqq x_i \leqq 1, \quad \text{or else} \quad 0 \leqq x_i \leqq 1/8\ ,$$

and this implies that indeed we have $(x_1,x_2,x_3,x_4) \in B$. This proves the inclusion (2.7).

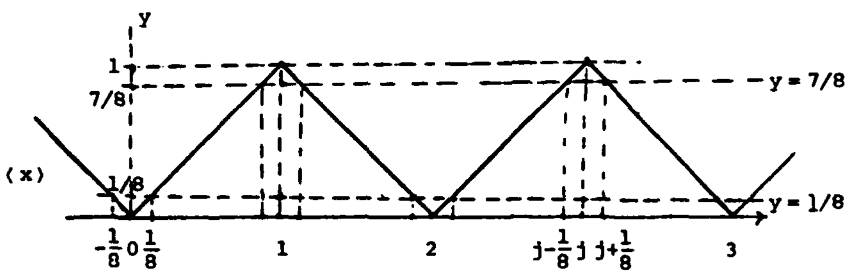

Fig. 3

However, if $u = 1/8$ say, then (2.1) show that $M_0 = (x_1,x_2,x_3,x_4)$ is the midpoint of the side A_0A_1, and by

$$M_0 = \left(\frac{1}{8}, \frac{1}{8}, \frac{3}{8}, \frac{5}{8}\right) \tag{2.8}$$

we conclude that M_0 is on the 2-facet $x_1 = 1/8$, $x_2 = 1/8$ of the hypercube $C_{3/8}$ defined by (2.2).

That a segment A_0A_1 may intersect the closed hypercube $\bar{C}_{3/8}$ in a single point (2.8) in the interior of its 2-facet

$$x_1 = 1/8,\ x_2 = 1/8,\ 1/8 \leqq x_3 \leqq 7/8,\ 1/8 \leqq x_4 \leqq 7/8\ .$$

is a peculiar property of R^4, which would not show well in the parallel projection of Fig. 2, nor in the 3-dimensional model which is also only a parallel projection of γ_4 on R^3. For this reason we do not show $C_{3/8}$ in Fig. 2, nor in the corresponding

3-dimensional model. Similarly, A_1A_2 touches $C_{3/8}$ in a single point M_1 of its 2-facet $x_2 = 1/8$, $x_3 = 1/8$.

For a proof of Statement 3 we refer to [3], or to [4, (4.5)].

A last word on the rectilinear construction of the vertices A_i in Fig. 2. In the 3-facet $x_4 = 0$ we have marked the four points P, Q, R, and S. Clearly $P = (1,1,0,0)$, $R = (0,1,1,0)$, and therefore their midpoint is $Q = (1/2,1,1/2,0)$. Finally, the midpoint A_3 of QS, with $S = (1,0,0,0)$, has the coordinates $A_3 = (3/4,2/4,1/4,0)$ which agrees with the value given by (2.5).

3. <u>The case $k = 2$</u>. Fig. 4 below is to be viewed as a 3-dimensional figure; it shows a parallel projection of the hypercube

(3.1) $$\gamma_4 = \{0 \leq x_i \leq 1;\ i = 1,2,3,4\}$$

onto our space R^3.

Let

(3.2) $$f, f', g, g' ,$$

be four parallel 2-dim facets of γ_4, so that f and f' are symmetric in the center $c = (1/2,1/2,1/2,1/2)$, and therefore so are g and g'. Without loss of generality we may choose the facets (3.2) to be

(3.3) $$\begin{aligned} f &= \{x_1 = 0,\ x_2 = 0\}, \quad & f' &= \{x_1 = 1,\ x_2 = 1\} , \\ g &= \{x_1 = 0,\ x_2 = 1\}, \quad & g' &= \{x_1 = 1,\ x_2 = 0\} . \end{aligned}$$

Let A be the center of f, and A' the center of f'. Furthermore, let BB' be a diagonal of g, and let CC' be the diagonal of g' which is not parallel to BB'. Finally, <u>let $\mathcal{O}$ denote the surface of the (skew) octahedron having the three diagonals</u>

(3.4) $$AA',\ BB',\ CC'$$

The 12 edges of $\mathcal{O}$ are marked by heavy lines in Fig. 4, but the reader is asked to regard $\mathcal{O}$ as being in R^4. A simple enumeration shows that there are 24 different octahedra , all congruent to each other.

Our main result is

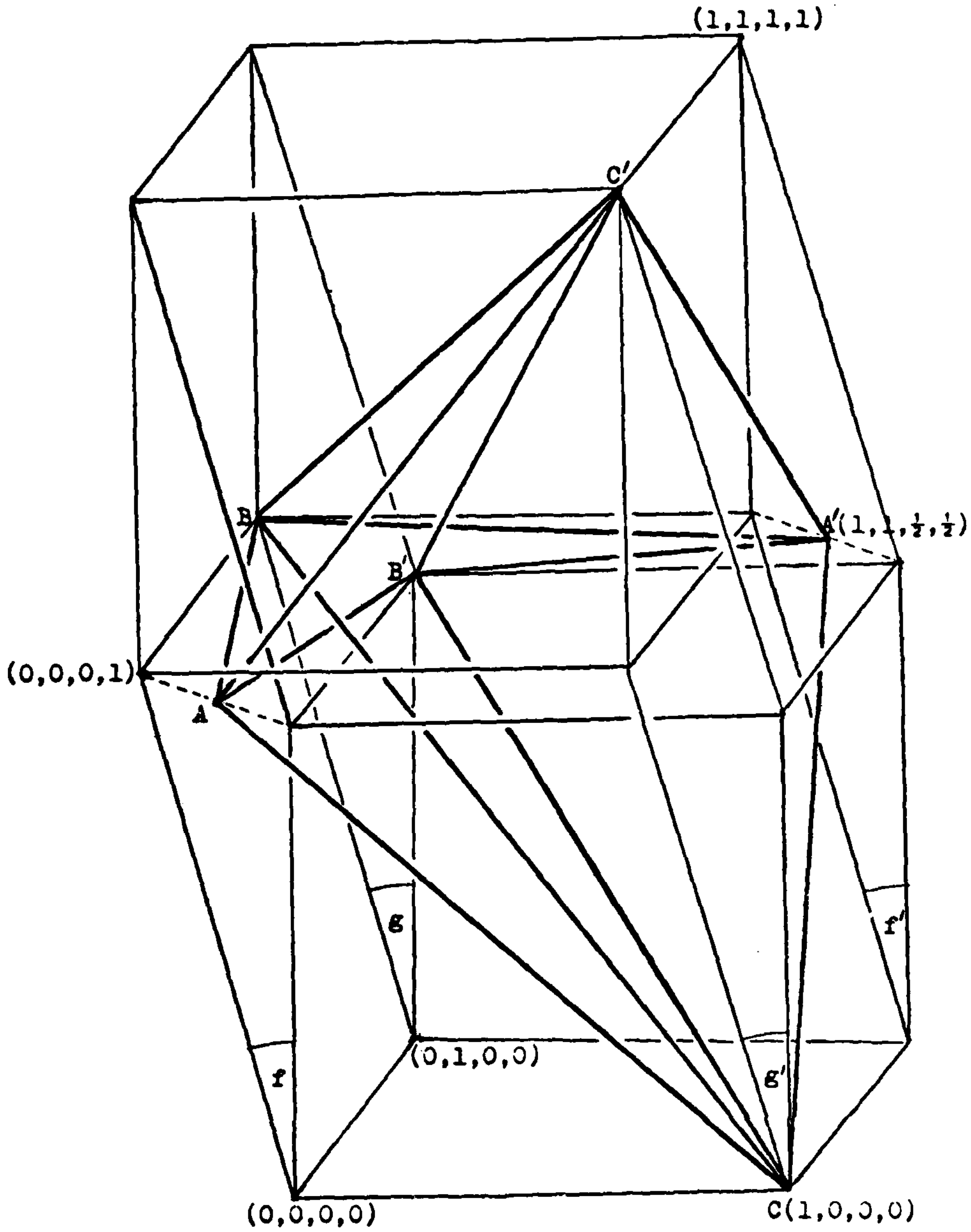

Fig. 4

Theorem 2. (i) The octahedron $\mathcal{O}$ is self-reflecting. This means that the 12 edges of $\mathcal{O}$ are in the boundary $\partial\gamma_4$, and that the entire surface of $\mathcal{O}$ is obtained by starting from one of its facets, for instance the triangle ABC, and reflecting it successively in the 3-facets of γ_4.

(ii) The four 2-facets of $\mathcal{O}$ having the common vertex A are congruent isosceles right-angled triangles, the four angles at A being all of 90°. The same is true of the four 2-facets with the common vertex A', where the four angles are all of 90°. The lengths of the sides of these eight triangles are

$$\sqrt{3/2},\ \sqrt{3/2},\ \sqrt{3}\ . \tag{3.5}$$

(iii) The octahedron $\mathcal{O}$ has no point in common with the open hypercube

$$C_{1/4}\ :\ \|x - c\|_\infty < \frac{1}{4}\ , \qquad \left(c = \left(\frac{1}{2}, \frac{1}{2}, \frac{1}{2}, \frac{1}{2}\right)\right)\ , \tag{3.6}$$

but each of its eight 2-facets touch a 1-facet of $C_{1/4}$ in a single point, namely its midpoint. Thus the facet ABC touches the 1-facet

$$x_1 = \frac{1}{4},\quad x_2 = \frac{1}{4},\quad x_3 = \frac{1}{4},\quad \frac{1}{4} < x_4 < \frac{3}{4} \tag{3.7}$$

in the single point $x_1 = 1/4$, $x_2 = 1/4$, $x_3 = 1/4$, $x_4 = 1/2$. This point of contact is obtained in Fig. 4 as follows: If M is the midpoint of the hypotenuse BC then the point (1/4, 1/4, 1/4, 1/2) is the midpoint of AM. Similarly for the reamining seven facets of $\mathcal{O}$.

Remark. Observe that for $k = 2$ and $n = 4$, the right side of (1.9) becomes $\frac{1}{2} - \frac{k}{2n} = \frac{1}{4}$. This strongly suggests the conjecture that $\rho_{2,4} = 1/4$, but this has not been established.

A proof of Theorem 2 requires some ideas and results fully developed in [4] which we need here for the special case of $n = 4$. For this reason we present them here independently of [4].

4. Monochromes and 4-Chromes in R^2.

Let

$$\{x\} = \min_{m\in\mathbb{Z}} |x - m| \tag{4.1}$$

denote the distance from the real x to the nearest integer. Its graph is also a zig-zag curve related to $\langle\cdot\rangle$ by $\{x\} = \langle 2x\rangle/2$.

If $\lambda_1 u_1 + \lambda_2 u_2 + a$ is a nonconstant linear function, then the equation $\{\lambda_1 u_1 + \lambda_2 u_2 + a\} = 0$ is equivalent with the infinite set of equations

$$\lambda_1 u_1 + \lambda_2 u_2 + a = j \quad (j \in \mathbb{Z}) . \tag{4.2}$$

Clearly (4.2) define in the (u_1,u_2)-plane a sequence of parallel and equidistant lines, the distance between two consecutive lines, or period, being $p = ((\lambda_1)^2 + (\lambda_2)^2)^{-1/2}$. However, if δ is a constant such that

$$0 < \delta < 1 , \tag{4.3}$$

then the inequality

$$M(\delta) : \{\lambda_1 u_1 + \lambda_2 u_2 + a\} \leq \frac{\delta}{2} , \tag{4.4}$$

defines an infinite system of parallel and equidistant strips

$$j - \frac{\delta}{2} \leq \lambda_1 u_1 + \lambda_2 u_2 + a \leq j + \frac{\delta}{2} \quad (j \in \mathbb{Z}) , \tag{4.5}$$

again with the period $p = ((\lambda_1)^2 + (\lambda_2)^2)^{-1/2}$, the common width w of the strips (4.5) being $w = \delta p$. The ratio

$$w/p = \delta \tag{4.6}$$

is called <u>the density of the set</u> $M(\delta)$ of strips. The set $M(\delta)$ is called a <u>monochrome of density</u> δ. $M(\delta)$ reminds us of the colored strips of an awning used to provide shade for store fronts, and we like to think of the strips (4.5) as carrying the same color γ, which explains the term <u>monochrome</u>.

<u>Example 1.</u> In Fig. 5 we see the set of vertical strips marked with the letter M_1. As their period is $p = 1$, and their width $w = 1/2$, we see that they form a monochrome $M_1(\frac{1}{2})$, of density $\delta = 1/2$. The inequality defining $M_1(\frac{1}{2})$ is clearly

$$M_1\left(\frac{1}{2}\right) : \left\{u_1 - \frac{1}{2}\right\} \leq \frac{1}{4} . \tag{4.7}$$

Now suppose that we have <u>four</u> monochromes

$$M_i(\delta) : \{\lambda_1^i u_1 + \lambda_2^i u_2 + a_i\} \leq \frac{\delta}{2} , \quad (i = 1,2,3,4) , \tag{4.8}$$

all of the same density δ, where we think of the strips of $M_i(\delta)$ as carrying the same color γ_i. We further assume that no two among the monochromes (4.8) are parallel, a condition expressed by requiring that

(4.9) <u>the</u> 4×2 <u>matrix</u> $\|\lambda_j^i\|$ <u>has no vanishing minor of order</u> 2 .

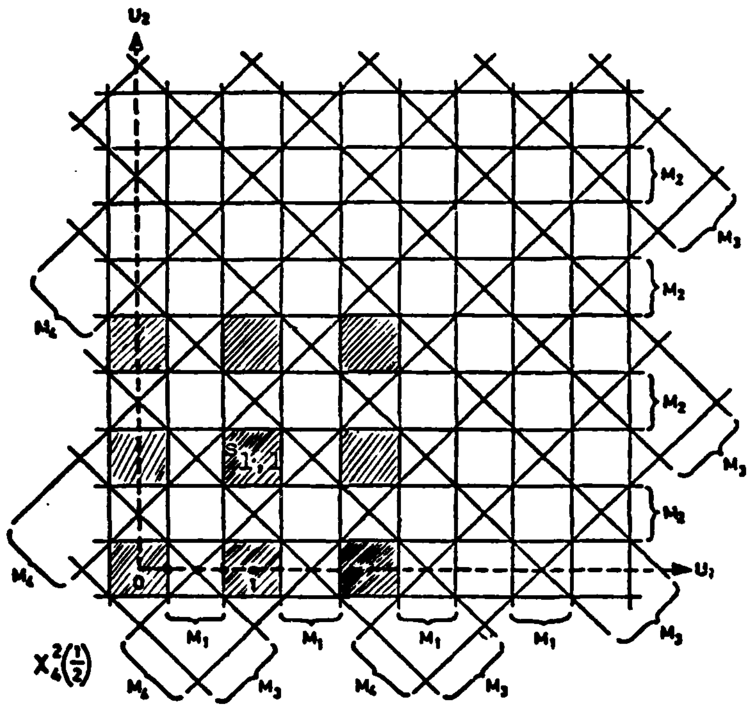

Fig. 5

<u>Definition 1.</u> <u>We say that the monochromes (4.8]) from a 4-chrome</u>

(4.10)
$$\chi_4^2(\delta) = \{M_1(\delta), M_2(\delta), M_3(\delta), M_4(\delta)\}$$

<u>of density</u> δ, <u>provided that the entire plane is covered with paint, hence that</u>

(4.11)
$$\bigcup_{i=1}^{4} M_i(\delta) = R^2 .$$

<u>Example 2.</u> Our Fig. 5 exhibits a 4-chrome $\chi_4^2(\frac{1}{2})$, which is the basis of our discussion. Here $M_1(\frac{1}{2})$ is the monochrome of our Example 1. $M_2(\frac{1}{2})$ is horizontal and defined by the inequality $\{u_2 - \frac{1}{2}\} \leq \frac{1}{4}$. The union $M_1(\frac{1}{2}) \cup M_2(\frac{1}{2})$ already covers the entire plane with the exception of the open squares

(4.12) $\quad s_{p,q} = \{p - \frac{1}{4} < u_1 < p + \frac{1}{4},\ q - \frac{1}{4} < u_2 < q + \frac{1}{4}\}$, where $(p,q) \in Z^2$,

centered at the lattice points and having sides = 1/2. They are hatched in Fig. 5. Notice that $M_3(\frac{1}{2})$ covers all squares $s_{p,q}$ such that $p + q$ is an <u>even</u> number, while $M_4(\frac{1}{2})$

covers all squares such that $p + q$ is <u>odd</u>. The inequalities (4.8) for the monochromes of Fig. 5 are explicitly given by

$$(4.13)\qquad \begin{aligned} M_1(\tfrac{1}{2}) &: \{u_1 - \tfrac{1}{2}\} \leq \tfrac{1}{4}, \\ M_2(\tfrac{1}{2}) &: \{u_2 - \tfrac{1}{2}\} \leq \tfrac{1}{4}, \\ M_3(\tfrac{1}{2}) &: \{\frac{u_1 + u_2}{2}\} \leq \tfrac{1}{4}, \\ M_4(\tfrac{1}{2}) &: \{\frac{u_1 - u_2 + 1}{2}\} \leq \tfrac{1}{4}, \end{aligned}$$

as is readily verified by the explicit form (4.5).

5. <u>Construction of the Octahedron $\mathcal{O}$ of Theorem 1.</u>

We derive $\mathcal{O}$ from the inequalities (4.13) by the device of <u>replacing the function $\{\cdot\}$ by the linear Euler spline</u> $\langle\cdot\rangle$, and thereby define the equations

$$(5.1)\qquad \begin{aligned} x_1 &= \langle u_1 - \tfrac{1}{2} \rangle, \\ x_2 &= \langle u_2 - \tfrac{1}{2} \rangle, \\ x_3 &= \left\langle \frac{u_1 + u_2}{2} \right\rangle, \\ x_4 &= \left\langle \frac{u_1 - u_2 + 1}{2} \right\rangle. \end{aligned}$$

By the general principle used in deriving (1.4) we already know that (5.1) define a <u>self-reflecting</u> polytope in γ_4. Let us abbreviate (5.1) writing

$$(5.2)\qquad \langle x_i \rangle = f(u_1, u_2).$$

This is a doubly-periodic function with the period 4 in u_1 and in u_2. We also easily verify that

$$(5.3)\qquad f(u_1+2, u_2-2) = f(u_1,u_2),\ f(u_1-2, u_2+2) = f(u_1,u_2)\ .$$

The functions on the right sides of (1.5) are continuous in R^2; they are also linear functions except on the lines where their arguments assume integer values, where their first partial derivatives are discontinuous. These are four sets of parallel lines

$$(5.4)\qquad \begin{aligned} &u_1 = j + \tfrac{1}{2}\ , &&u_2 = j + \tfrac{1}{2} \\ &u_1 + u_2 = 2j\ , &&u_1 - u_2 = 2j - 1\ , \text{ for all integers } j\ . \end{aligned}$$

In Fig. 6 we draw the 4×4 square in the (u_1,u_2)-plane

$$(5.5)\qquad S = \{-\tfrac{1}{2} \le u_1 \le 4 - \tfrac{1}{2},\ -\tfrac{1}{2} \le u_2 \le 4 - \tfrac{1}{2}\}\ .$$

Drawing appropriate lines (5.4) we find that S is partitioned into 32 triangles indicated by solid lines.

From (5.1) we find by direct evaluations that the six points

$$(5.6)\qquad \begin{aligned} &A = f(\tfrac{1}{2}, \tfrac{1}{2}) = (0,\ 0,\ \tfrac{1}{2},\ \tfrac{1}{2})\ , &&A' = f(-\tfrac{1}{2}, -\tfrac{1}{2}) = (1,\ 1, \tfrac{1}{2},\ \tfrac{1}{2}) \\ &B = f(\tfrac{1}{2}, -\tfrac{1}{2}) = (0,\ 1,\ 0,\ 1)\ , &&B' = f(\tfrac{1}{2}, \tfrac{3}{2}) = (0,\ 1,\ 1,\ 0) \\ &C = f(-\tfrac{1}{2}, \tfrac{1}{2}) = (1,\ 0,\ 0,\ 0)\ , &&C' = f(\tfrac{3}{2}, \tfrac{1}{2}) = (1,\ 0,\ 1,\ 1) \end{aligned}$$

agree with the vertices of $\mathcal{O}$ as given in Fig. 4. We also label in Fig. 6 these six points with the letters $A, B, \ldots, C'$. Using the identities (5.3) it is easy to label all 25 points of Fig. 6 with the letter of the vertex of $\mathcal{O}$ into which they are mapped.

To get a clear picture of the mapping (5.2) it is convenient to consider the eight facets of $\mathcal{O}$

$$(5.7)\qquad \begin{aligned} &T_1 = A'BC,\ T_2 = ABC,\ T_3 = ABC',\ T_4 = A'BC'\ , \\ &T_5 = AB'C,\ T_6 = A'B'C,\ T_7 = AB'C',\ T_8 = A'B'C'\ . \end{aligned}$$

We also label each triangle of Fig. 6 with the symbol T_i of the facet into which it is mapped. In Fig. 6 we divide the square S into four 2×2 squares, and Fig. 6 shows that each of these 2×2 squares is mapped into the entire surface of $\mathcal{O}$:

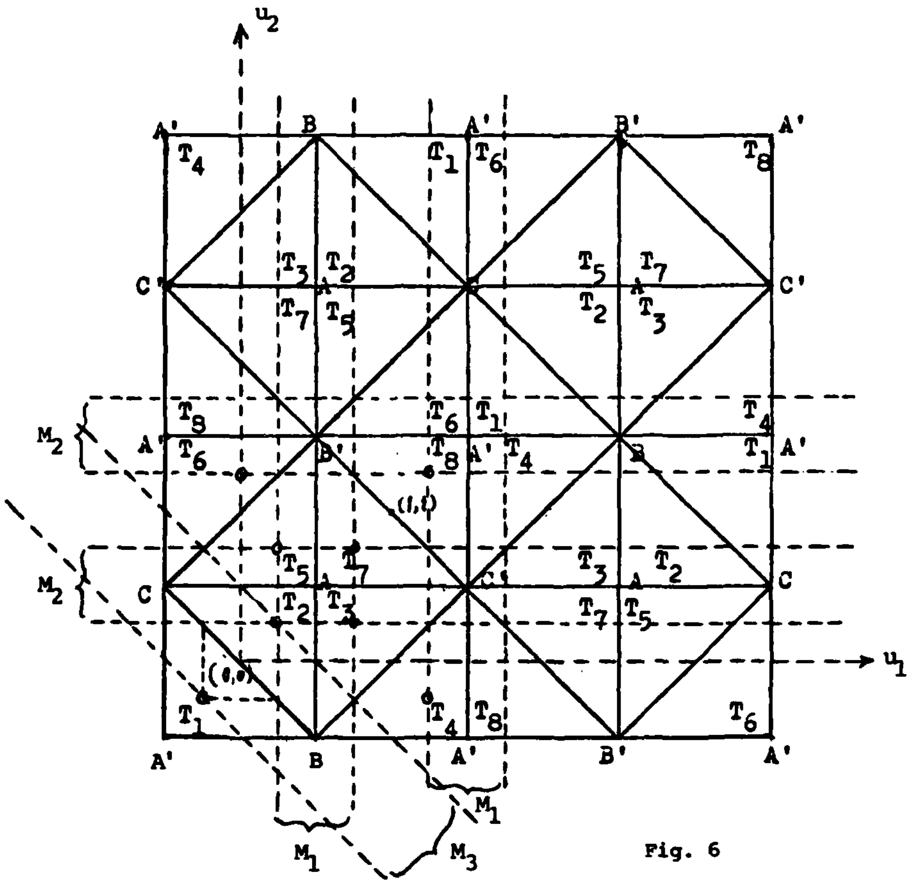

Fig. 6

<u>The Image of S by (5.2) covers $\mathcal{O}$ four times.</u>

Let us finally derive the values (3.5). Observing that $(d/dx)\langle x\rangle = \pm 1$, it follows that in the interior of the 32 triangles of Fig. 6 we may differentiate the functions (5.1) obtaining

$$dx_1 = \pm du_1,\ dx_2 = \pm\, du_2,\ dx_3 = \pm\, \frac{1}{2}\,(du_1 + du_2),\ dx_4 = \pm\, \frac{1}{2}\,(du_1 - du_2)\ .$$

It follows that

$$ds^2 = \sum_1^4 (dx_i)^2 = (du_1)^2 + (du_2)^2 + \frac{1}{4}\,(du_1 + du_2)^2 + \frac{1}{4}\,(du_1 - du_2)^2$$

whence

(5.8) $$ds^2 = \frac{3}{2}\left((du_1)^2 + (du_2)^2\right) .$$

This shows that our mapping from S to $\mathcal{O}$ is (locally) a similitude of ration $1 : \sqrt{3/2}$. This shows that the 8 triangles (5.7) are congruent to each other and that they are as described in (i) and (ii) of Theorem 2; also the values (3.5) are now verified. We believe to have amply demonstrated parts (i) and (ii) of Theorem 2.

6. Proof of Part (iii) of Theorem 2.

The proof has two parts:

1° We are to show that

(6.1) $$\mathcal{O} \cap C_{1/4} = \emptyset .$$

2° We are to determine the points of the intersection $\mathcal{O} \cap \overline{C_{1/4}}$.

Proof of 1°. We establish (6.1) in a way similar to the proof of the inclusion (2.7): We consider the closed box

(6.2) $$B_0 = \Upsilon_4 \setminus C_{1/4}$$

and wish to show that

(6.3) $$\mathcal{O} \cap B_0 .$$

Referring to Fig. 7 we state

Lemma 1. For a real x we have

(6.4) $$\{x\} \leq 1/4 ,$$

if and only if

(6.5) either $0 \leq \langle x\rangle \leq 1/4$, or else $3/4 \leq \langle x\rangle \leq 1$.

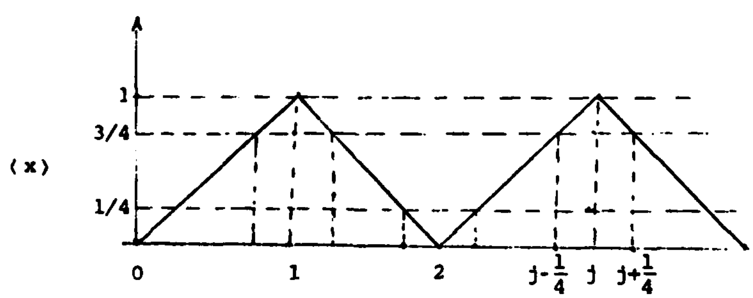

Fig. 7

A glance at Fig. 7 proves this. Now we use the fact that Fig. 5 represents a 4-chrome $Y_4^2(\frac{1}{2})$ whose four monochromes (4.13), of density $\frac{1}{2}$, cover the plane. But then for every (u_1,u_2) we have

$$(u_1,u_2) \in M_i(\tfrac{1}{2}), \quad \text{for some } i ,$$

and by Lemma 1 and (5.1) we conclude that for some i we have

$$\text{either } 0 \leq x_i \leq \tfrac{1}{4}, \text{ or else } \tfrac{3}{4} \leq x_i \leq 1 .$$

This establishes (6.3).

<u>Solution of 2°.</u> Here we use the peculiarly tight structure of the 4-chrome of Fig. 5. The answer, as described by the example of the 1-facet (3.7), follows from the following observations.

1'. On the two boundary lines of a strip of any of the monochromes (4.13), like $M_3(\frac{1}{2})$ sau. we have $\{(u_1 + u_2)/2\} = 1/4$.

2'. Every vertex of the squares $s_{p,q}$, of (4.12), is on the boundary lines of <u>three</u> monochromes. For instance, the point

$$u_1 = 1/4, \quad u_2 = 1/4 \tag{6.6}$$

is on the boundary lines of $M_1(\frac{1}{2})$, $M_2(\frac{1}{2})$, $M_3(\frac{1}{2})$, as shown by Fig. 5, or Fig. 6. From 1' and (5.1) it follows that the image of the point (6.6) is on the 1-facet

$$x_1 = \langle u_1 - \tfrac{1}{2}\rangle = \tfrac{1}{4},\ x_2 = \langle u_2 - \tfrac{1}{2}\rangle = \tfrac{1}{4},\ x_3 = \left\langle \frac{u_1 + u_2}{2}\right\rangle = \tfrac{1}{4} .$$

as is also easily verified.

Incidentally also Fig. 7 shows that $\{x\} = 1/4$ iff either $\langle x\rangle = 1/4$, or else $\langle x\rangle = 3/4$.

We have shown that every facet T_i, of $\mathcal{O}$, touches $\bar{C}_{1/4}$ in a single point having in T_i the barycentric coordinates $(1/2, 1/4, 1/4)$; these points are especially marked in Fig. 6.

<u>A Conjecture.</u> Fig. 5 suggests very strongly the following

<u>Conjecture 1.</u> <u>The density</u> $\delta = \frac{1}{2}$ <u>is the least possible density of a 4-chromo (4.10), hence satisfying the conditions (4.11) and (4.9).</u>

This is the simplest case (for $k = 2$ and $n = 4$) of the Conjecture 1' of [4, p.67].

Part II. The Case When $k = 3$

7. The Polytope SO_4.

The present Part II is based on and uses the results of [5]. We also abandon the hypercube (3.1) and consider instead the hypercube

(7.1) $$\gamma_4 = \{-1 \leq x_i \leq 1, \quad i = 1,2,3,4\}$$

having its side = 2.

The 4-dimensional analogue SO_4 of Kepler's Stella Octangula $SO = SO_3$, was studied in [5, Part IV, §9, p. 289]. It was found to be a connected 3-dimensional polytope Π_4 having as 3-facets 16 congruent regular tetrahedra and 16 congruent regular truncated tetrahedra. The shapes of these 3-facets are shown in Fig. 5 of [5, p. 289].

The 16 regular tetrahedra were shown in [5, §5] to be given by the intersections

(7.2) $$F_3(\varepsilon_1,\varepsilon_2,\varepsilon_3,\varepsilon_4) = \gamma_4 \cap \left\{ \sum_1^4 \varepsilon_i x_i = 3 \right\}, \quad \text{where} \quad \varepsilon_i = \pm 1 .$$

Also that the 16 regular truncated tetrahedra are given by

(7.3) $$F_1(\varepsilon_1,\varepsilon_2,\varepsilon_3,\varepsilon_4) = \gamma_4 \cap \left\{ \sum_1^4 \varepsilon_i x_i = 1 \right\}, \quad \text{where} \quad \varepsilon_i = \pm 1 .$$

The 32 polyhedra (7.2) and (7.3) are all inscribed in γ_4 in the following sense: All of their 2-facets are on the boundary $\partial\gamma_4$ of γ_4, i.e. they are in the eight cubes $x_i = \pm 1$ $(i = 1,\ldots,4)$.

Let π denote a hyperplane of R^4. The 2-facets of the intersection $\gamma_4 \cap \pi$ are the intersections of π with the 3-facets of γ_4; likewise the 1-facets of $\gamma_4 \cap \pi$ are the intersections of π with the 2-facets of γ_4. Let us determine the 1-facets of $\gamma_4 \cap \pi$, where π is one of the two hyperplanes

(7.4) $$\pi_3 : \sum_1^4 \varepsilon_i x_i = 3 ,$$

or

$$(7.5) \qquad \pi_1 : \sum_1^4 \varepsilon_i x_i = 1 .$$

For this purpose we select the 2-facet of γ_4 given by

$$(7.6) \qquad f = \{x_1 = \eta_1,\ x_2 = \eta_2, \ \text{where} \ \eta_1 = \pm 1,\ \eta_2 = \pm 1\} .$$

From (7.4) and (7.6) we find that $f \cap \pi_3$ is defined (within γ_4) by the three equations $x_1 = \eta_1$, $x_2 = \eta_2$, and

$$(7.7) \qquad \varepsilon_3 x_3 + \varepsilon_4 x_4 = 3 - \varepsilon_1\eta_1 - \varepsilon_2\eta_2 .$$

This last equation depends on the values of η_1, η_2, and becomes

$$\varepsilon_3 x_3 + \varepsilon_4 x_4 = \begin{cases} 3 & \text{if } \ \varepsilon_i \eta_i \ \text{ are of opposite signs} \\ 1 & \text{if } \ \varepsilon_1\eta_1 = \varepsilon_2\eta_2 = 1 \\ 5 & \text{if } \ \varepsilon_1\eta_1 = \varepsilon_2\eta_2 = -1 . \end{cases}$$

However, the first and third equations have evidently no solutions in γ_4, and we are left with the equations

$$x_1 = \varepsilon_1,\ x_2 = \varepsilon_2,\ \varepsilon_3 x_3 + \varepsilon_4 x_4 = 1 .$$

Likewise we find $f \cap \pi_1$ to be described by $x_1 = \eta_1$, $x_2 = \eta_2$ and

$$\varepsilon_3 x_3 + \varepsilon_4 x_4 = 1 - \varepsilon_1\eta_1 - \varepsilon_2\eta_2 ,$$

or

$$\varepsilon_3 x_3 + \varepsilon_4 x_4 = \begin{cases} 1 & \text{if } \ \varepsilon_i \eta_i \ \text{ are of opposite signs ,} \\ -1 & \text{if } \ \varepsilon_1\eta_1 = \varepsilon_2\eta_2 = 1 \\ 3 & \text{if } \ \varepsilon_1\eta_1 = \varepsilon_2\eta_2 = -1 . \end{cases}$$

Here the last has no intersection with γ_4 and the final result is as follows: <u>All 1-facets of $f \cap \gamma_4$ are given by</u>

$$(7.8) \qquad x_1 = \eta_1,\ x_2 = \eta_2,\ \varepsilon_3 x_3 + \varepsilon_4 x_4 = 1$$

<u>for</u> $\varepsilon_3 = \pm 1$, $\varepsilon_4 = \pm 1$.

The equations (7.8) are evidently the four sides of the square having as vertices the successive midpoints of the four sides of the (square) 2-facet (7.6) of γ_4. We reach a similar conclusion if we replace in (7.6) x_1 and x_2 by x_i and $x_j (i < j)$. We have proved

<u>Theorem 3.</u> γ_4 <u>has</u> $6 \times 4 = 24$ <u>square 2-facets. In each of these squares we inscribe the square with vertices in successive midpoints of its sides. The sides of these inscribed squares give</u> $4 \times 24 = 96$ <u>segments, and these 96 segments are all the 1-facets of</u> SO_4.

8. A Description of Fig. 8.

Like Figures 2 and 4 Fig. 8 shows a parallel projection of γ_4 on our R^3. In view of our new definition of γ_4, the lower cube is $x_4 = -1$ and the upper cube in $x_4 = 1$. No attempt was made to draw all 96 1-facets of SO_4 of Theorem 3, as this would have overburdened our Fig. 8, rather we exhibit only four of the 32 3-facets of SO_4, which are connected by three successive reflexions.

We start from the tetrahedron

(8.1) $$F_3(1,1,1,1) = ABCD .$$

It is in γ_4, but its four 2-facets are in four of the 3-facets of γ_4: Thus

(8.2) $$BCD \subset \{x_4 = 1\} ;$$

indeed, Fig. 8 shows clearly that BCD belongs to the top cube. (8.1) is reflected by each of the four 3-facets of γ_4 which contain its four 2-facets. However, we choose to reflect (8.1) only in the 3-facet $x_4 = 1$. To do this reflexion we rewrite (see (7.2)) $x_1 + x_2 + x_3 + x_4 = 3$ as

$$x_1 + x_2 + x_3 + (x_4 - 1) = 2 ,$$

and change the sign of the fourth term on the left, obtaining the new equation

$$x_1 + x_2 + x_3 - (x_4 - 1) = 2$$

or

$$x_1 + x_2 + x_3 - x_4 = 1$$

obtaining the new 3-facet

(8.3) $$F_1(1,1,1,-1) .$$

From (7.3) we see that (8.3) is in the hyperplane $x_1 + x_2 + x_3 - x_4 = 1$, and we wish to

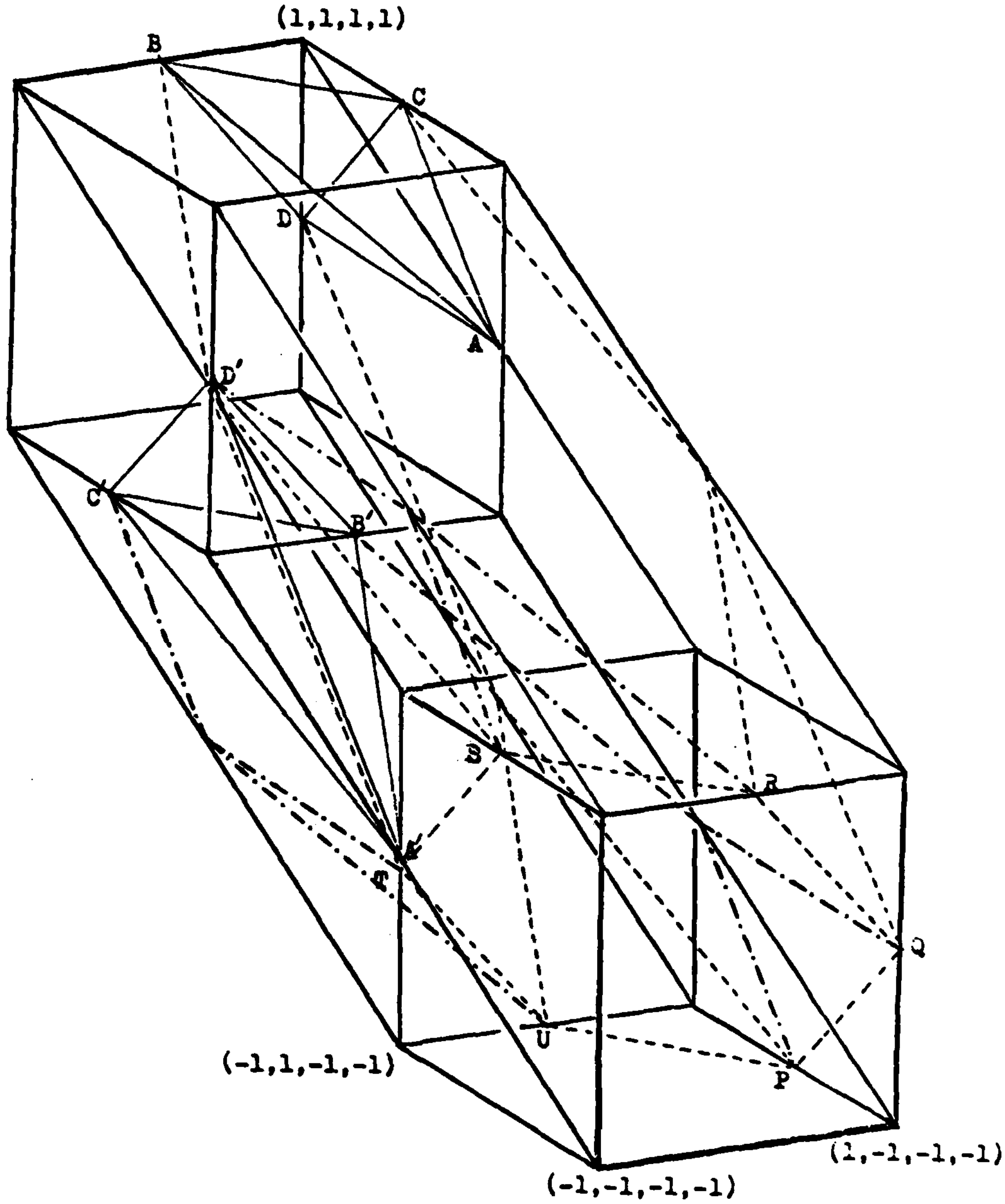

Fig. 8

reflect it in $x_4 = -1$. To do this we rewrite it as $x_1 + x_2 + x_3 - (x_4 + 1) = 0$, and change the sign of the 4th term to obtain

$$x_1 + x_2 + x_3 + (x_4 + 1) = 0 ,$$

or $-x_1 - x_2 - x_3 - x_4 = 1$. Again by (7.3) we see that we have reached the 3-facet

$$F_1(-1,-1,-1,-1) . \tag{8.4}$$

Our final reflexion is again in the top cube $x_4 = 1$: We rewrite $-x_1 -x_2 - x_3 - x_4 = 1$ as $-x_1 - x_2 - x_3 - (x_4 - 1) = 2$ and changing the sign of its 4th term we have $-x_1 - x_2 - x_3 + (x_4 - 1) = 2$, which is equivalent to $-x_1 - x_2 - x_3 + x_4 = 3$. By (7.2) this gives our last 3-facet

$$F_3(-1,-1,-1,1) . \tag{8.5}$$

By (8.1), (8.3), (8.4), and (8.5) we obtain the string of four 3-facets of SO_4:

$$F_3(1,1,1,1) \cup F_1(1,1,1,-1) \cup F_1(-1,-1,-1,-1) \cup F_3(-1,-1,-1,1) , \tag{8.6}$$

which we now attempt to represent in Fig. 8.

The first is given by (8.1). The second, $F_1(1,1,1,-1)$ is a truncated tetrahedron having as top 2-facet the triangle BCD, and as bottom 2-facet the regular hexagon

$$PQRSTU . \tag{8.7}$$

Its remaining 2-facets are three triangles and three hexagons, which are affine regular, and are indicated by "dashed" lines. The third 3-facet, $F_1(-1,-1,-1,-1)$ has also as bottom 2-facet the hexagon (8.7), while its top 2-facet is the triangle B'C'D', also belonging to $x_4 = 1$. Its remaining 2-facets are also three triangles and three hexagons shown by "dash-dot-dash" lines. The last term of (8.6) is the tetrahedron

$$F_3(-1,-1,-1,1) = A'B'C'D' . \tag{8.8}$$

Let me say that the 3-dimensional model of Fig. 8 shows much more clearly the two truncated tetrahedra (8.3) and (8.4), also because their edges are pointed in different colors.

The following "optical" remark might help to illuminate the situation: If we place a light-bulb in the interior of ABCD so that its rays spread within the 3-flat determined by ABCD, then its rays strike $x_4 = 1$ in the triangle BCD, get reflected by $x_4 = 1$ into (8.3), filling it and striking $x_4 = -1$ in the hexagon (8.7). These rays are reflected by $x_4 = -1$ into (8.4). Finally, these rays again strike $x_4 = 1$ in B'C'D', and are reflected into the tetrahedron (8.8). Notice that the extreme points A and A' are symmetric in the center c of γ_4.

Our final remark is that the 32 3-facets of SO_4 fall apart into 8 strings of polyhedra, like the union (8.6), as follows. For $\varepsilon_i = \pm 1$ we assume that

$$\varepsilon_1 \varepsilon_2 \varepsilon_3 \varepsilon_4 = 1 . \tag{8.9}$$

In place of (8.1) we now start with the tetrahedron

$$F_3(\varepsilon_1, \varepsilon_2, \varepsilon_3, \varepsilon_4) \tag{8.10}$$

and perform the reflexions in $x_4 = \varepsilon_4$, $x_4 = -\varepsilon_4$, and finally in $x_4 = \varepsilon_4$. These operations, as described before, lead to the union

$$F_3(\varepsilon_1, \varepsilon_2, \varepsilon_3, \varepsilon_4) \cup F_1(\varepsilon_1, \varepsilon_2, \varepsilon_3, -\varepsilon_4) \cup F_1(-\varepsilon_1, -\varepsilon_2, -\varepsilon_3, -\varepsilon_4) \cup F_3(-\varepsilon_1, -\varepsilon_2, -\varepsilon_3, \varepsilon_4) . \tag{8.11}$$

Varying the ε_i subject to (8.9) gives eight unions like (8.11), and together they contain all distinct 32 3-facets fo SO_4. If we disregard the restriction (8.9), we would obtain each 3-facet twice.

Bollelaan 10

Naarden, North Holland

REFERENCES

1. D. König and A. Szücs, Mouvement d'un point abandonné a l'intérieur d'un cube, Rendiconti del Circ. Mat. diPalermo, 38(1913), 79-90.

2. I. J. Schoenberg, Extremum problems for the motion of a billiard ball I. The L_p-norm, $1 \leq p < \infty$, Indag. Math., 38(1976), 66-75.

3. ______________, Extremum problems for the motion of a billiard ball II. The L_∞-norm Indag. Math., 38(1976), 263-279.

4. ______________, Extremum problems for the motions of a billiard ball III. The multi-dimensional case of König and Sžucs, Studia Scie. Math. Hungarica, 13(1978), 53-78.

5. ______________, Extremum problems for the motions of a billiard ball IV. A higher-dimensional analogue fo Kepler's Stella Octangula, Studia Scie. Math. Hungarica, 14(1979), 273-292.

6. ______________, Mathematical Time Exposures, a book soon to be published by the Mathematical Association of America.

IJS/ed

SECURITY CLASSIFICATION OF THIS PAGE (When Data Entered)

REPORT DOCUMENTATION PAGE		READ INSTRUCTIONS BEFORE COMPLETING FORM
1. REPORT NUMBER 2467	2. GOVT ACCESSION NO. AD-A127 726	3. RECIPIENT'S CATALOG NUMBER
4. TITLE (and Subtitle) SELF-REFLECTING SKEW POLYGONS AND POLYTOPES IN THE 4-DIMENSIONAL HYPERCUBE		5. TYPE OF REPORT & PERIOD COVERED Summary Report - no specific reporting period
		6. PERFORMING ORG. REPORT NUMBER
7. AUTHOR(s) I. J. Schoenberg		8. CONTRACT OR GRANT NUMBER(s) DAAG29-80-C-0041
9. PERFORMING ORGANIZATION NAME AND ADDRESS Mathematics Research Center, University of Wisconsin 610 Walnut Street Madison, Wisconsin 53706		10. PROGRAM ELEMENT, PROJECT, TASK AREA & WORK UNIT NUMBERS Work Unit Number 1 - Applied Analysis
11. CONTROLLING OFFICE NAME AND ADDRESS U. S. Army Research Office P.O. Box 12211 Research Triangle Park, North Carolina 27709		12. REPORT DATE January 1983
		13. NUMBER OF PAGES 24
14. MONITORING AGENCY NAME & ADDRESS(if different from Controlling Office)		15. SECURITY CLASS. (of this report) UNCLASSIFIED
		15a. DECLASSIFICATION/DOWNGRADING SCHEDULE

16. DISTRIBUTION STATEMENT (of this Report)

Approved for public release; distribution unlimited.

17. DISTRIBUTION STATEMENT (of the abstract entered in Block 20, if different from Report)

18. SUPPLEMENTARY NOTES

19. KEY WORDS (Continue on reverse side if necessary and identify by block number)

Extremum problems, billiard ball motions

20. ABSTRACT (Continue on reverse side if necessary and identify by block number)

The papers [2,3,4,5] of the list of References dealt with the following extremum problem: In the hypercube γ_n of R^n we have a k-flat L_k in general position which is reflected by the $(n - 1)$-facets of γ_n, while we continue indefinitely reflecting these reflexions, thereby generating a finite

DD FORM 1473 1 JAN 73 EDITION OF 1 NOV 65 IS OBSOLETE

UNCLASSIFIED

SECURITY CLASSIFICATION OF THIS PAGE (When Data Entered)

ABSTRACT (cont.)

or infinite polytope Π_n^k. Here we assume that

$$1 \leqq k \leqq n - 1 .$$

The present paper deals with the case when $n = 4$, and when

(1) $$k = 1,\ k = 2, \text{ and } k = 3 .$$

The main problem is to determine Π_n^k to stay away as much as possible from the center c of γ_n, the main emphasis being the graphic representation of the extremum Π_n^k. This is done for the three cases (1) in Figures 2, 4, and 8. These figures are parallel projections of γ_4 onto our space R^3. The author also made for each of these figures 3-dimensional models made of thin wooden sticks, and my colleagues, in the Fine Arts Department of UW, say that these models qualify as examples of Constructive Art. All of these polygons and polytopes are <u>self-reflecting</u>, meaning thereby that we obtain the entire object by starting from one of its k-facets, and reflecting it successively in the facets of γ_4.

END

FILMED

6-83

DTIC